Greek Letters

ψ = correcting factor of the component liquid molar flowrate
σ = correcting factor of the component vapor molar flowrate
θ = theta multiplier

Superscripts

U = referred to a liquid-side stream
W = referred to a vapor-side stream
$*$ = theta parameter used in the proposed methodology

Subscripts

ca = calculated value
co = corrected value
f = feed tray number
i,k = component index
j,l,m,p,q = tray number
np = bottom tray

LITERATURE CITED

Billingsley, D. S., "On the numerical solutions of Problems in Multicomponent Distillation of the Steady State II," *AIChE J.*, **16**, 3 (1970).

Boston, J. F., and S. L. Sullivan, Jr., "An improved Algorithm for Solving Mass Balance equations in Multistage Separation Processes," *Can. J. of Chem. Eng.*, **50**, 664 (1972).

Fredenslund, A., J. Gmehling, and P. Rasmussen, "Vapor-Liquid Equilibria Using UNIFAC," Elsevier, Amsterdam (1977).

Gallun, S. E., and C. D. Holland, "Solve more Distillation Problems. Part 5. For Highly Non Ideal Solutions," *Hydrocarbon Processing*, **55**, 6 (1976).

Hayden, J. G., and J. P. O'Connel, "A Generalized Method for Predicting Second Virial Coefficients," *Ind. Eng. Chem. Process Des. Dev.*, **14**, 3 (1975).

Henley, E. J., "Equilibrium stage Separation Operations in Chem. Engineering," Wiley, N.Y.

Hess, F. E., S. E. Gallun, S. E. Bentzen, and G. W. Holland, "Solve more Distillation Problems. Part 8: Which Method to Use," *Hydrocarbon Processing*, **56**, 6 (1977).

Holland, C. D., "Multicomponent Distillation," Prentice-Hall Inc., Englewood Cliffs, NJ (1963).

Holland, C. D., and P. T. Eubank, "Solve more Distillation Problems. Part 2: "Partial molar enthalpies calculated," *Hydrocarbon Processing*, **53**, 11 (1974).

Holland, C. D., and P. G. Pendon, "Solve more Distillation Problems. Part 1. Improvements give Exact Answer," *Hydrocarbon Processing*, **53**, 7 (1974).

Holland, C. D., and M. S. Kuk: "Solve more distillation problems. Evaluate existing columns," *Hydrocarbon Processing*, **54**, 7 (1975).

Holland, C. D., G. P. Pendon, and S. E. Gallum, "Solve more distillation problems. Part 3: Application to absorbers," *Hydrocarbon Processing*, **54**, 1 (1975).

Lyster, W. N., S. L. Sullivan, D. S. Billingsley, and C. D. Holland, "Figure distillation This new way. Part 1: New Convergence Method will Handle Many cases," *Petroleum Refiner*, **38**, 6 (1975).

Pierucci, S. J., E. M. Ranzi, G. E. Biardi, and M. Dente, "T-method computes distillation," *Hydrocarbon processing*, **60**, 9 (1981).

Reid, R. C., J. M. Prausnitz, and T. K. Sherwood, "The properties of Gases and Liquids," McGraw Hill, 3rd ed. (1977).

Soave, G., "Equilibrium Constants from a modified Redlich-Kwong equation of State," *Chem. Eng. Sci.*, **27**, 1197 (1972).

Wang, J. C., and G. E. Henke, "Tridiagonal matrix for distillation," *Hydrocarbon Processing*, **45**, 155 (1966).

Manuscript received March 26, 1981; revision received February 11, and accepted March 4, 1982.

A Residence-Time Model for Trickle-Flow Reactors Incorporating Incomplete Mixing in Stagnant Regions

A model for the liquid-phase residence time in a trickle-flow reactor has been derived and experimentally verified using a tracer input. The model, termed the Ideal Plug Flow Stagnancy Model, postulates that the prime liquid-phase dispersive mechanism in such reactors is the interchange between the dynamic and stagnant regions. Unlike previous models, however, it does not require the assumption of perfect mixing in the stagnant zones. While the results of the study confirm that the mixing is incomplete, they show clearly that back mixing rather than molecular diffusion is the dominant exchange mechanism.

KIN-MUN KAN and P. F. GREENFIELD

Department of Chemical Engineering
University of Queensland
St. Lucia, Qld, 4067, Australia

SCOPE

Trickle-bed catalytic reactors find applications in situations where it is necessary or expedient to contact a gas and a liquid phase in a fixed-bed reactor. Such reactors are usually operated in the cocurrent mode to allow high flowrates of liquid and gas, which would cause flooding in countercurrent situations. Of course, cocurrent operation implies that the gas-liquid transfer resistance is not rate-limiting. The boundary between the gas and liquid phases is not fixed, but fluctuates in a highly complex manner as the fluids interact in finding their way through the packed bed.

Not surprisingly, the commercial design of trickle-bed reactors is based on extensive pilot plant and existing commercial

Kin-Mun Kan is presently at the Ampol Research Laboratories, Lytton, Qld, Australia.

plant data, a procedure which is costly and time-consuming. While there have been some attempts at a design based on theoretical principles, this approach is still limited by an inadequate understanding of the hydrodynamics of the fluid phases, particularly the liquid phase. It is generally recognized that only a portion of the liquid phase at any particular time is dynamic.

The existing models which describe the residence-time distribution of the liquid phase are generally of two classes. Either, they attribute all dispersive effects to a single parameter, the axial dispersion coefficient $\overline{E}_z$, or they assume that the dispersion is caused by interchange between the dynamic and stagnant regions of the liquid phase. Matsuura et al. (1976) combined both of these effects, but showed the dominance of the latter. A key assumption in the crossflow stagnancy models is that the stagnant zone is perfectly mixed, an assumption which has not been tested and which seems unrealistic given the assumed fluid characteristics. This work aims to develop and experimentally verify a model which describes the liquid-phase distribution for small catalyst packings. The model incorporates the above concepts but does not rely on the assumption of perfect mixing in the stagnant regime. Such a model, when incorporated with a reaction term, leads naturally to a trickle-bed reactor model.

CONCLUSIONS AND SIGNIFICANCE

A three-parameter model has been developed to describe the liquid-phase residence time for trickle flows through a packed-bed reactor with small packings. The model partitions the liquid phase into a dynamic regime and a stagnant regime, with the dynamic portion being in plug flow and with mass interchange occurring between the two. Unlike previous models, a concentration profile was assumed in the stagnant zone with the rate of interchange being controlled by a parameter, E'_s. This parameter will tend towards the molecular diffusivity of a species, if molecular diffusion is the dominant transport mechanism in the stagnant regions and towards infinity if the regions are perfectly mixed. The three parameters in the model are the total holdup, h_t; the fraction of this holdup that is dynamic, ϕ; and a dimensionless group, Sg, which reflects the transport between the dynamic and stagnant regions and which includes E'_s. A solution of the model equations in the Laplace domain was developed.

The model was verified experimentally for small packings; it was shown that the model accurately predicted the response to a pulse input. The parameters were estimated from the experimental data by the method of cumulants and regression techniques. The cumulants technique was found to be satisfactory, but, using numerical inversion, a set of parameters could always be found that better described the experimental data. The holdup, h_t, compared well with the values obtained by direct measurement.

The parameters ϕ and Sg were found to be independent of the individual fluid-phase Reynolds numbers. The constancy of ϕ (0.73 ± 0.08, 95% confidence limits) is consistent with the rivulet theory of liquid flow through the packed bed. The constancy of Sg (0.13 ± 0.02, 95% confidence limits) implies that the stagnant zone dispersion coefficient, E'_s, is proportional to the superficial liquid velocity. In turn, this means that although the stagnant regions are not perfectly mixed, backmixing rather than molecular diffusion dominates the transport process. This conclusion was further verified when similar values of E'_s were obtained with a tracer of much higher molecular diffusivity.

The success of the model adds further evidence to the conclusion that interchange between the stagnant and dynamic regions of the liquid phase is the dominant dispersive mechanism in trickle-bed reactors. Incorporating an appropriate reaction rate expression into the above model will allow the performance of a trickle-bed reactor to be predicted.

EXISTING RESIDENCE-TIME MODELS

The simplest model used to describe the liquid-phase residence time in a trickle-flow reactor is the Ideal Plug Flow Model in which every liquid element flowing through the system has exactly the same residence time. In real systems, dispersive effects cause a spread of residence times. In the Axially Dispersed Plug Flow Model, which is widely accepted (Furzer and Michell, 1970), the true nature of the liquid flow is ignored. The concentration distribution is described by:

$$\frac{\partial c}{\partial t} = \overline{E}_z \frac{\partial^2}{\partial z^2} - U_d \frac{\partial c}{\partial z} \tag{1}$$

where

$$U_d = \overline{U}_L / h_t, \tag{2}$$

and all dispersive effects are attributed to the axial dispersion coefficient, $\overline{E}_z$.

Michell and Furzer (1972) showed statistically that the model could not account for the dispersive effects adequately. The same conclusion was drawn by Hoogendoorn and Lips (1965), Bennett and Goodridge (1970), as well as Van Swaaij et al. (1969) who pointed out that the Axially Dispersed Plug Flow Model gives too early a breakthrough and insufficient tailing. The lack of good fit of the experimental data to the model is probably due to the absence of any consideration of the nature of the liquid flow through the packed bed. In particular, the long tailing of the liquid-phase residence-time data indicates that there are liquid regions which considerably slow down a proportion of the liquid elements.

Thus, liquid holdup in a trickle bed may be considered to consist of two different regimes, one which is essentially stagnant (stagnant holdup) and the other which is moving (dynamic holdup). Dynamic holdup, so defined, is different from the classical dynamic or operating holdup which is the fraction of liquid that drains from the bed after all flows have been terminated. Likewise, the stagnant holdup is different from the classical static holdup.

Hoogendoorn and Lip (1965) introduced a model, termed the Ideal Crossflow Model, in which the sole cause of dispersion is the interchange of mass between the dynamic and stagnant regions. The liquid-phase flowing in the dynamic region is considered to be in ideal plug flow while the stagnant region is completely mixed. A mass transfer coefficient, k, is the constant of proportionality for the rate of mass transfer in the same manner as for gas absorption studies. The model leads to a set of partial differential equations:

$$\frac{\partial c}{\partial t} = -U_d \frac{\partial c}{\partial z} - \frac{N a_s}{\phi h_t} \tag{3}$$

where

$$Na_s = ka_s(c_d - c_s) = h_t(1-\phi)\frac{c_s}{\partial t}, \quad (4)$$

c_d and c_s being the concentrations in the dynamic and stagnant regions respectively. The three parameters are ϕ, which represents the dynamic fraction of the total holdup, k, the coefficient for mass transfer between the dynamic and stagnant regions and, h_t, the total holdup. Hoogdendoorn and Lips (1965) estimated these parameters using countercurrent flow data in beds of large packings. The model was extended to cocurrent flows by Hochman and Effron (1969).

Van Swaaij et al. (1969), and Bennett and Goodridge (1970) independently proposed an additional parameter to account for axial dispersion in the dynamic region. The four-parameter Dispersed Crossflow Model is given by:

$$\frac{\partial c}{\partial t} = E_z'\frac{\partial^2 c}{\partial z^2} - U_d\frac{\partial c}{dz} - \frac{Na_s}{\phi h_t}, \quad (5)$$

where E_z' in this case refers only to the dispersion in the dynamic liquid region. Matsuura et al. (1976) extended the Dispersed Crossflow Model to cocurrent flows and assessed the relative importance of the two dispersion mechanisms by comparing the Peclet number obtained by using the Axially Dispersed Plug Flow Model with that obtained by using the Dispersed Cross-Flow Model. They were able to conclude that stagnant regions contribute nearly 90% of the total dispersion at moderate liquid flowrates.

The true nature of the stagnant phase may be resolved by examining the mechanism of the mass transfer between the dynamic and the stagnant regions. A key to this mechanism is the role of the molecular diffusivity of the tracer used in residence-time studies. If the mass transfer is by molecular diffusion, then the mass transfer rate should be proportional to the molecular diffusivity of the tracer; or, more appropriately, the coefficient of dispersion for the dispersive flux into the stagnant region must be equal to the molecular diffusivity of the tracer. On the other hand, if the mechanism is by eddy mixing, then the molecular diffusivity of the tracer plays an insignificant role in the mass transfer, and the coefficient of dispersion would, in fact, be a function of the liquid flowrate which determines the degree of agitation causing the eddy mixing. The results of the few works reported so far in the literature have been conflicting. This aspect has been investigated experimentally in this work.

In developing a realistic model of the residence-time characteristics in a trickle-bed reactor, it is useful to consider the structure of the liquid phase in its flow through the bed. Davidson et al. (1959) adopted a film theory to explain holdup in which the liquid phase is considered to flow in thin films over the packing surfaces. This theory has also been adopted for the prediction of holdup and pressure drop by Buchanan (1971) and Hutton and Leung (1975). Davidson (1962) extended the model to account for dispersion with limited success. Although the film theory is attractive in being amenable to analytical solution techniques, it assumes a flow pattern which is highly simplified and probably unrealistic.

Porter and Stephens (1969) considered a rivulet model in which the liquid phase flows preferentially in distinct paths or channels. Michell and Furzer (1972) commented that with the rivulet theory, the liquid flowrate must be proportional to the number of rivulets, each of which wets a certain area of packing surface. As such, the rivulet theory requires the wetted area to be proportional to the liquid flowrate, which contradicts experimental observations. At the same time, assuming that the rivulets are nearly identical to each other, the residence time would be independent of the flowrate, which again contradicts experimental observations. However, these contradictions would not arise if the rivulet size is not constant. In a real situation, it is likely that a mixed state exists with both rivulets and films being present in a range of physical sizes. The rivulet theory unfortunately cannot easily be verified by experimental observations or be described quantitatively.

None of the mathematical models reported in the literature take into account the phenomenon of multiple hydrodynamic states which has been discussed elsewhere (Kan & Greenfield, 1978, 1979; Kan, 1980). Briefly, it has been observed for beds of small packings that the pressure drop and holdup for a given set of fluid flowrates depend on the previous history of gas flowrates. This phenomenon has been attributed to surface tension effects of the liquid phase in the bed causing the gas flowpaths to be oriented in the general direction of flow when a higher flowrate is achieved. This orientation is retained even when the gas flowrate is reduced, affecting the pressure drop and holdup. The earlier work did not indicate how the liquid-phase residence time was affected by this phenomenon.

In this paper, a model is proposed that incorporates a more realistic description of the mass transfer across the stagnant region than do the existing models. The model is similar to the Crossflow Models of Hoogendoorn and Lips (1965), Hochman and Effron (1969), Van Swaaij et al. (1969), Bennett and Goodridge (1970) and Matsuura et al. (1976), except that mixing in the stagnant holdup is not necessarily complete. The transport mechanism may be solely by molecular diffusion or only partly so, with eddy mixing playing an important role. A similar mechanism for describing mass transport in open channel flow was proposed by Hays (1966).

MODEL DEVELOPMENT

Consider an elemental section of a trickle bed as shown in Figure 1. The thickness of the section is Δz which may be taken as thin as possible; it is situated at a distance z from the top of the bed. The fractional volume of this elemental section occupied by the liquid phase is h_t, the total liquid holdup; the dynamic fraction of this is ϕ.

For dispersion in the dynamic region in the z-direction, the dispersive mass flux is proportional to the product of the concentration gradient and a transverse area which may be taken to be

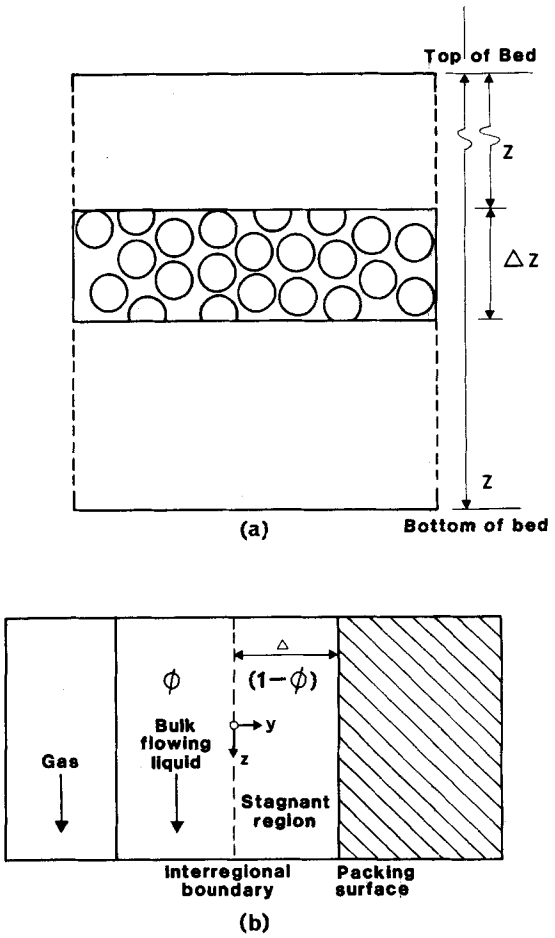

Figure 1. An elemental section of trickle-flow reactor and schematic diagram of proposed model.

the area covered by the dynamic holdup, $\phi h_t A$, where A is the cross-sectional area of the bed. The constant of proportionality is the axial dispersion coefficient, E_z'.

For mass transfer in the stagnant region, the distance, y, in the stagnant region is measured from the boundary with the dynamic region. A Fickian-type relationship is used:

$$\frac{\partial c_s}{\partial t} = E_s' \frac{\partial^2 c_s}{\partial y^2}, \tag{6}$$

where c_s is the concentration in the stagnant region. The mass flux at any time t is then given by:

$$N_s = -E_s' \left.\frac{\partial c_s}{\partial y}\right|_{y=0} \tag{7}$$

E_s' represents another constant of proportionality. If the mechanism of migration of chemical species in the stagnant regions is by molecular diffusion, E_s' equals D_M, the molecular diffusivity. In general, however, some eddy mixing is involved. An imaginary interregional boundary may be drawn, although in reality the boundary is not precise. It is also convenient to designate an area of interregional mass transfer, a_s, expressed in units of area per unit volume of bed.

A mass balance over the elemental section yields the equation:

$$\frac{\partial c_d}{\partial t} = E_z' \frac{\partial^2 c_d}{\partial z^2} - U_d \frac{\partial c_d}{\partial z} + \frac{a_s E_s'}{\phi h_t} \left.\frac{\partial c_s}{\partial y}\right|_{y=0} \tag{8}$$

where

$$U_d = \frac{Q_L}{\phi h_t A} = \frac{\bar{U}_L}{\Delta h_t} \tag{9}$$

Equation 8 is in fact the equation of motion for the dynamic region of the Dispersed Crossflow Model (Eq. 5).

A simplification may be introduced by relating the surface area of interregional mass transfer, a_s, to the total holdup and the parameter ϕ by assuming a simple geometry for the stagnant region. For a slab geometry,

$$a_s \Delta = (1 - \phi) h_t, \tag{10}$$

where Δ is the stagnant "film" thickness, a dimension that occurs in one of the boundary conditions and is a measure of the distance from the boundary between the stagnant and dynamic regions and the solid packing surface. The error introduced in this simplifying assumption depends on the degree of deviation of the true geometry of the stagnant region from the assumed slab geometry, and is reflected in the parameters determined with the model. However, the error is not serious if the parameters estimated from one packed bed are applied to another bed in which the stagnant region geometry is the same. The current study is concerned with beds of small packings; the parameters determined with this simplification in the model should be applicable to other beds of small packings in which the liquid stagnant geometry is similar.

With such an approximation, the equation of motion becomes:

$$\frac{\partial c_d}{\partial t} = E_z' \frac{\partial^2 c_d}{\partial z^2} - U_d \frac{\partial c_d}{\partial z} + \frac{(1 - \phi)}{\phi \Delta} E_s' \left.\frac{\partial c_s}{\partial y}\right|_{y=0} \tag{11}$$

At the interface between the dynamic and stagnant regions,

$$y = 0, \quad c_d = c_s \quad \text{for all } z \tag{12}$$

For an impulse input signal,

$$t = 0, \quad z = 0; \quad c_d = \delta(t), \quad \bar{c}_d = 1 \tag{13}$$

$$t = 0, \quad z > 0; \quad c_d = 0, \quad c_s = 0 \tag{14}$$

Since the signal must eventually decay to zero as it moves down the reactor,

$$z \to \infty; \quad c_d \to 0 \quad \text{for all } t. \tag{15}$$

The mathematical model as expressed by Eqs. 6 and 11 is termed the Dispersed Plug Flow Stagnancy Model and is identical to the Dispersed Crossflow Model in terms of the equation of motion for the dynamic region. The only difference lies in the assumption of partial mixing in the stagnant region.

The Dispersed Plug Flow Stagnancy model contains four parameters. Considerable difficulty is encountered in obtaining reliable estimates of each of these parameters from the response of a column to an impulse input signal. A simplification may be applied based on the results of previous studies (Matsuura et al., 1976), which showed that dispersion caused by mass transfer between the stagnant and dynamic regions is more important than that contributed by the eddy mixing effect in the dynamic region; the other alternative of neglecting the stagnant region results in the Axially Dispersed Plug Flow Model which has been shown to be inadequate in modelling trickle flows.

Starting with Eq. 11, if the axial dispersion coefficient E_z' is assumed zero, the following equation results:

$$\frac{\partial c_d}{\partial t} = -U_d \frac{\partial c_d}{\partial z} + \frac{a_s E_s'}{\phi h_t} \left.\frac{\partial c_s}{\partial y}\right|_{y=0} \tag{16}$$

MODEL SOLUTION

Equations 6 and 16 may be expressed in dimensionless form:

$$\frac{\partial C_s}{\partial \phi} = \frac{h_t}{P_M} \frac{\partial^2 C_s}{\partial \eta^2} \tag{17}$$

$$\frac{\partial C_D}{\partial \theta} = -\frac{1}{\phi} \frac{\partial C_D}{\partial \xi} + \frac{(1 - \phi) h_t}{\phi \dfrac{\Delta}{Z} P_M} \left.\frac{\partial C_s}{\partial \eta}\right|_{\eta=0} \tag{18}$$

where

$$C_s = c_s/c_o, \quad C_D = c_d/c_o, \quad \theta = \phi U_D t/Z$$

$$\xi = z/Z, \quad \eta = y/Z, \quad P_M = \bar{U}_L Z/E_s'$$

and c_o is such that

$$\int_0^\infty C_D d\theta = 1 \tag{19}$$

The solution to Eqs. 17 and 18 is given in the Laplace domain by:

$$\bar{C}_D = \exp\left\{-\phi s - \frac{(1 - \phi)}{\dfrac{\Delta}{Z}} \sqrt{h_t s/P_M} \tanh \frac{\Delta}{Z} \sqrt{P_M s/h_t}\right\} \tag{20}$$

It is noted that h_t, Δ and E_s' are related in a fixed manner in the form of $\Delta/Z \sqrt{P_M/h_t}$ and are apparently, therefore, not independent parameters. In actual fact, h_t is independent through its relationship to θ and C_o. The dimensionless group that relates these parameters is termed the Stagnancy number (Sg), i.e.

$$Sg = \Delta \sqrt{\bar{U}_L/E_s' Z} \tag{21}$$

The Ideal Plug Flow Stagnancy Model is preferred over the Dispersed Plug Flow Stagnancy Model because of the difficulty in obtaining reliable estimates of the four parameters from residence time data. Although the Laplace transform domain solution for the Ideal Plug Flow Stagnancy Model is still too complicated for analytical inversion, it is in the simpler form of the product of two exponential terms, one of which is $(-\phi h_t A/\bar{U}_L)$. This means that the inversion can be carried out on

$$\left[\exp\left\{-\frac{(1 - \phi)\sqrt{h_t s}}{Sg} \tan h\, Sg \sqrt{s/h_t}\right\}\right]$$

with the former term representing a lag time.

The method of weighted cumulants was used to obtain first estimates of the parameters from residence time data. Ostergaard and Michelson (1969) suggested the use of weighted moments to handle such data. They are defined as follows:

$$\omega_k = \int_0^\infty t^k e^{-st} c dt = (-1)^k \frac{d^k \bar{c}(s)}{ds^k} \tag{22}$$

The zeroth weighted moment is in fact the Laplace transform of $c(t)$. Anderssen and White (1971) pointed out that no simple relationship exists between the input, output and system weighted moments for a linear flow system and proposed the use of weighted cumulants, as follows:

$$K_o(s) = ln\ \omega_o(s) \tag{23}$$

$$K_{k+1}(s) = -d/ds K_k(s) \tag{24}$$

Anderssen and White (1971) also proposed an expression for the optimum weighting factor, S_{opt}:

$$S_{opt} = \frac{2k_{av}}{(t_{mode,in} + t_{mode,out} - \Delta t_D)} \tag{25}$$

For the Ideal Plug Flow Stagnancy Model, i.e., Eq. 20, the zeroth cumulant is:

$$K_0 = ln\ \overline{C}_D$$

$$= -\phi s - \alpha\sqrt{s}\ tanh\ \beta\sqrt{s}$$

where

$$\alpha = \frac{(1-\phi)\sqrt{h_t}}{Sg}$$

$$\beta = Sg/\sqrt{h_t}$$

The higher order cumulants are given by:

$$K_1 = \phi + \tfrac{1}{2}\alpha s^{-1/2} tanh\ \beta\sqrt{s} + \tfrac{1}{2}\alpha\beta\ sech^2\ \beta\sqrt{s} \tag{27}$$

$$K_2 = \tfrac{1}{4}\alpha s^{-3/2} tanh\ \beta\sqrt{s} - \tfrac{1}{4}\alpha\beta s^{-1}\ sech^2\ \beta\sqrt{s} + \tfrac{1}{2}\alpha\beta^2 s^{-1/2}\ sech^2\ \beta\sqrt{s}\ tanh\ \beta\sqrt{s} \tag{28}$$

The parameters in the model may be estimated from experimental residence time data by solving a set of n equations in n unknowns, formed by equating the analytical expressions for the cumulants with the numerically computed values, i.e.:

$$K_{i,theoretical} = K_{i,experimental} \quad i = 0,\ n-1 \tag{29}$$

As the expressions for the cumulants are nonlinear, a numerical technique was necessary to solve for the parameters. The method adopted was that of Hooke & Jeeves using an adaptation of the computer program published in Carnahan, Luther and Wilkes (1969).

The model equations were solved for an ideal pulse input signal because of mathematical convenience. In practice, the input signal was not well defined but could be measured and reproduced with high accuracy. Correction for the non-ideality of the input signal was made to the numerically-derived residence time distribution using the Convolution Theorem, as follows:

$$g(t) = \int_0^t g(t-\tau)C(\tau)d\tau \tag{30}$$

where $f(t)$ is the input signal, $C(t)$ is the response for an ideal pulse input, and $g(t)$ is the actual response, which may be determined by numerical integration.

For the method of cumulants, a very simple relationship exists between the input and output signals:

$$K_{k,SYS} = K_{k,OUTPUT} - K_{k,INPUT} \tag{31}$$

For an ideal input signal, $K_{k,INPUT}$ is zero.

The parameters estimated by the method of cumulants were used as the starting values in a nonlinear regression routine which aimed to minimize the square error area between the observed and predicted results. It was generally found that improved estimates could be obtained in this fashion. Full details of the above procedure may be found in Kan (1980).

EXPERIMENTAL

The trickle-bed equipment used for the experimental work is shown schematically in Figure 2.

Water was pumped into the system by a twin-piston metering pump. To eliminate pressure pulsations, the water entered the packed bed via an air-pressurized chamber. Air was fed cocurrently and entered the bed through the annular region around the liquid distributor.

The packed column consisted of flanged sections made up from 25-mm ID acrylic tubing; the length of the reactor was varied from 500 to 800 mm. The packings were glass spheres of 0.5 and 1.0 mm in diameter.

The gas flowrates ranged from 0.01 to 1.85 $kg \cdot m^{-2} \cdot s^{-1}$ (Re_G from 6.1 to 100). The particle Reynolds number for the liquid phase ranged from 0.5 to 10.2.

There was a need for treatment of the experimental data prior to actual analysis. The raw experimental data had to be made dimensionless at some stage so as to be consistent with the model equations. Additionally, a reasonable cut-off point had to be nominated for the front and tail portions of the response curve where the signal merged with the background noise and could provide no useful information. Finally, a slight instrumental drift that resulted in a small but perceptible change in the base line had to be corrected.

The analysis of the residence time data by the method of cumulants was

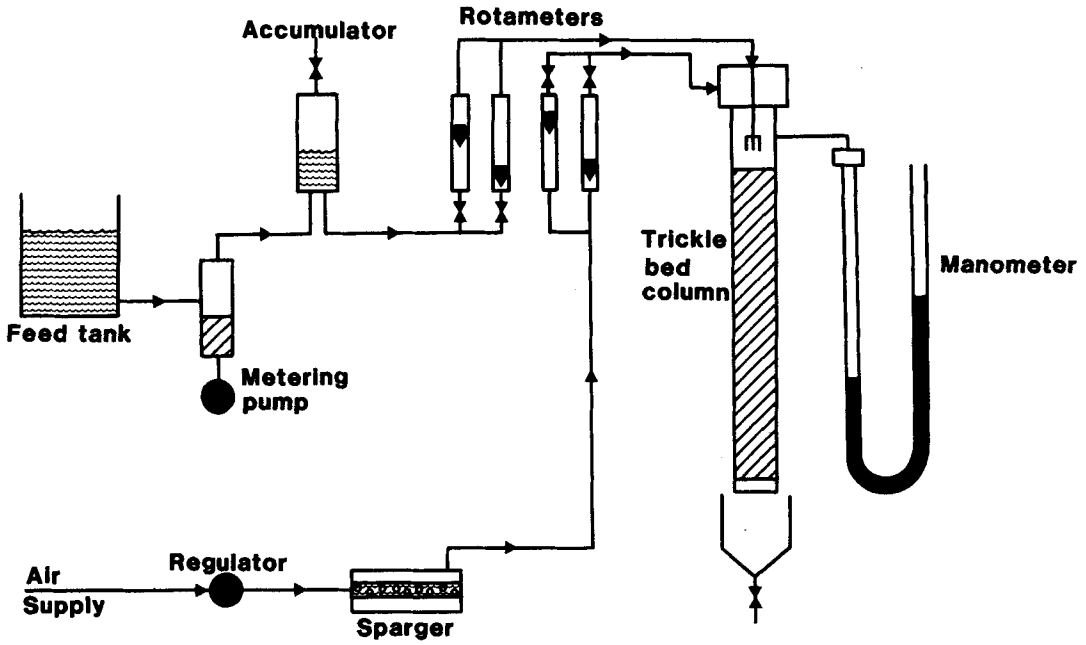

Figure 2. Experimental trickle-flow reactor.

TABLE 1. SUMMARY OF PARAMETER ESTIMATION RESULTS

Re_L	Re_G	Re_{Gmax}	h_t Measured Directly	h_t from Zeroth, First Moment	Parameters h_t	ϕ	Sg	Error Area
1.0	7.5	7.5	0.160	0.166	0.143	0.75	0.1113	0.066
1.0	12.2	12.2	0.148	0.168	0.142	0.70	0.1103	0.109
1.0	80.5	80.5	0.096	0.124	0.098	0.74	0.097	0.086
1.0	12.2	80.5	0.148	0.179	0.155	0.72	0.124	0.029
1.0	7.5	102	0.160	0.195	0.175	0.716	0.131	0.068
1.0	100	100	0.089	0.183	0.095	0.736	0.100	0.136
1.0	55.5	80.5	0.104	0.103	0.113	0.770	0.168	0.162
1.0	32.4	80.5	0.118	0.149	0.122	0.750	0.120	0.180
10.2	12.2	12.2	0.237	0.253	0.222	0.720	0.102	0.077
10.2	42.2	42.2	0.188	0.201	0.181	0.740	0.107	0.078
10.2	12.2	42.2	0.240	0.249	0.222	0.730	0.114	0.063
0.49	35.8	35.8	0.128	0.172	0.131	0.75	0.140	0.184
0.493	6.1	35.8	0.190	0.247	0.204	0.72	0.140	0.071
0.493	6.1	6.1	0.190	0.225	0.179	0.64	0.13	0.078
5.1	9.35	9.35	0.267	0.268	0.213	0.75	0.14	0.104
5.1	6.1	6.1	0.286	0.303	0.257	0.71	0.171	0.100
5.1	6.2	12.7	0.286	0.310	0.255	0.67	0.145	0.082
5.1	2.55	12.7	0.333	0.343	0.288	0.850	0.140	0.139
0.493*	6.1*	6.1*	0.190	0.242	0.195	0.793	0.149	0.150

* Dextran as tracer.

carried out after normalisation. The normalized concentration C'_D is defined as:

$$\int_0^\infty C'_D\, dt = 1 \tag{32}$$

where time t is measured in seconds.

RESULTS AND DISCUSSION

The results of the computations are summarized in Table 1; the results shown represent the average of a number of replicate runs carried out at each set of conditions. A typical experimental residence time curve and the corresponding curve based on the solution of the model is shown in Figure 3. The goodness of fit between the model predictions and the experimental observations is expressed in terms of the area that lies between the two curves, Table 1.

A reliable check on an estimated parameter is its consistency with the value determined independently by other methods. Such a check is possible only in respect to the total holdup, h_t, which may be directly measured as well as estimated from the zeroth and first moments as shown below:

$$h_t = m_1 Q_L / m_0 V_R \tag{33}$$

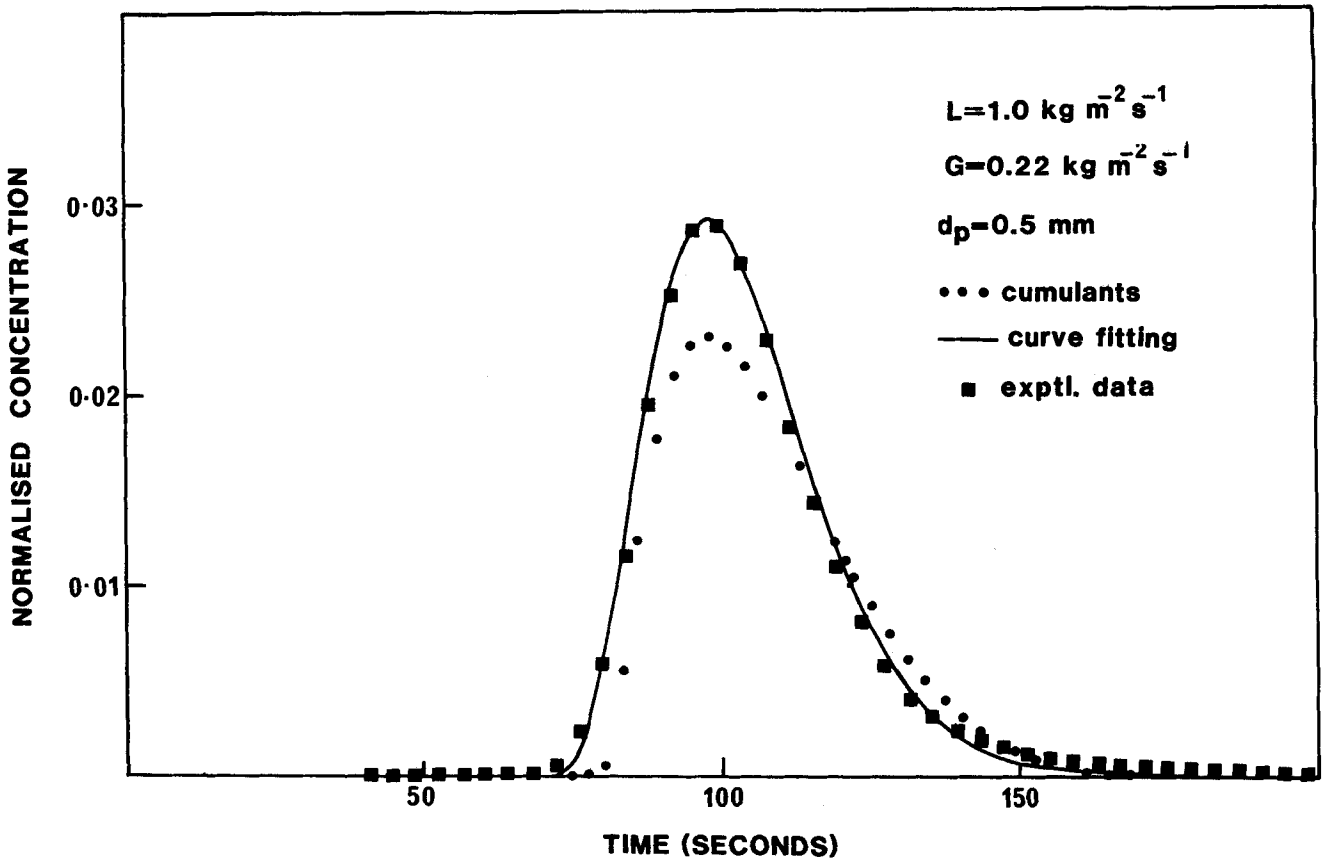

Figure 3. Typical residence-time distribution.

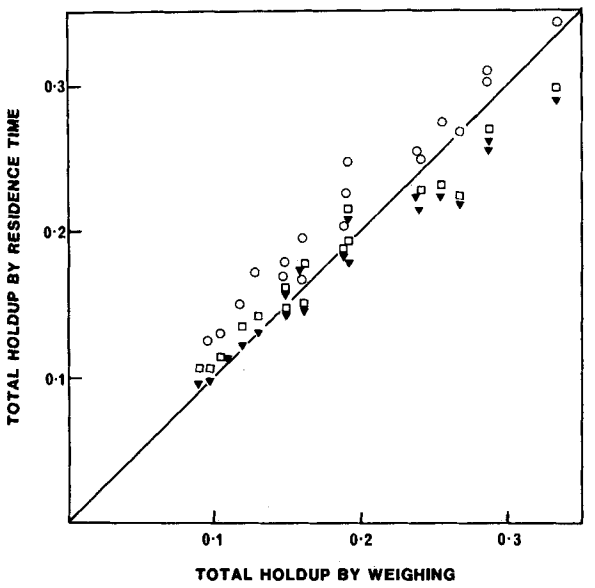

Figure 4. Comparison of holdup values determined by various methods. ○ zeroth and first moments; □ cumulants method; ▼ curve fitting (numerical inversion) method.

where m_0, m_1 are the zeroth and first moments, respectively, Q_L the liquid flowrate, and V_R the volume of the bed.

Figure 4 compares the holdup determined by the different techniques and shows that they are, on the whole, quite consistent. The total holdup determined by direct measurement is considered to be the most accurate. The results by the cumulants and curve-fitting methods compare well, but, for some unknown reason, the deviation appears to be higher for holdups calculated from the zeroth and first moments even though these are normally associated with less error than the second-order cumulants used in the cumulants method.

The relationship,

$$h_t = 8.5\,\mathrm{Re}_L^{0.15}\mathrm{Re}_G^{-0.25}\mathrm{Re}_{G_{max}}^{0.014} \tag{34}$$

was obtained with a multiple correlation coefficient of 0.96 and an F-value of 55.6. It is interesting to compare this relationship with that obtained by direct measurement. Liquid holdup from the same column as used in the residence time study has been correlated by the method of Specchia and Baldi (1977) in the form:

$$\frac{h_t}{\epsilon} = 14.9\,\mathrm{Re}_L^{0.30}\mathrm{Ga}_L^{-0.35} \tag{35}$$

where

$$\mathrm{Ga}_L = d_p^3\rho_L\left(\rho_L g + \left(\frac{-\Delta p}{Z}\right)\right)/\mu_L^2 \tag{36}$$

However, the Galileo number, Ga_L, contains a pressure drop term which has to be replaced by an expression in fluid Reynolds numbers. The simplified form of Turpin and Huntington (1967),

$$f_{RLG} = 4273\,\mathrm{Re}_L^{0.49}\mathrm{Re}_G^{-1.02}\mathrm{Re}_{G_{max}}^{-0.25} \tag{37}$$

where

$$f_{RLG} = -\left(\frac{\Delta p}{Z}\right)d_p\epsilon/[3\rho_G\overline{U}_G^2(1-\epsilon)] \tag{38}$$

has been found to be most suitable since it retains linearity in the relationship to be developed. Noting that except for very low gas flowrates,

$$|\rho_L g| \ll \left|\left(\frac{-\Delta p}{Z}\right)\right|$$

a simple relationship between liquid holdup and the fluid Reynolds numbers only can be obtained:

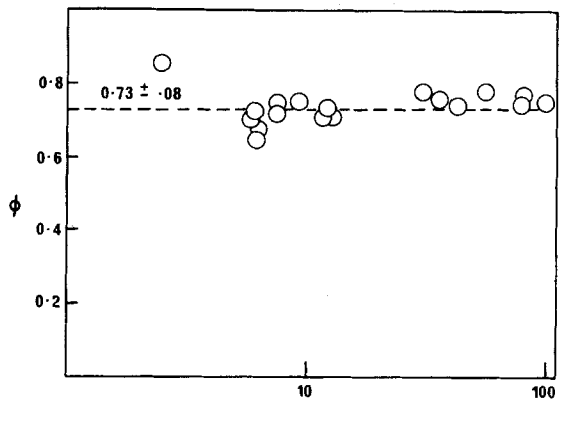

Figure 5. Relationship between ϕ and gas-phase Reynolds number.

$$h_t = \left[\epsilon\frac{0.193\mu_L^2\epsilon\rho_G}{\rho_L\mu_G^2(1-\epsilon)}\right]^{0.358}\mathrm{Re}_L^{0.12}\mathrm{Re}_G^{-0.35}\mathrm{Re}_{G_{max}}^{0.09} \tag{39}$$

Since the first term of Eq. 39 is constant except at high gas flowrates, it is reasonable to compare the exponents of the remaining terms with those of Eq. 34. The agreement between the two equations in the exponents of Re_G and Re_L is excellent considering the widely different techniques used. The difference in the exponents of $\mathrm{Re}_{G_{max}}$ is quite considerable although the confidence limits on this parameter are quite wide.

Correlations similar to that of Eq. 34 were also attempted on ϕ and Sg but the results in both instances were negative, indicating that, within the error limits, the parameters were in fact independent of the flow conditions in the range considered in the experiments.

The mean value obtained for the parameter ϕ was 0.73 with a standard deviation of 0.04 which gives a reasonably small 95% confidence interval of ±0.08. A plot of ϕ against the gas phase particle Reynolds number is shown in Figure 5. It is stressed that the plotted points include a wide range of liquid Reynolds numbers confirming the insensitivity of ϕ to flowrates. When considered in relation to the models developed to explain the multiple hydrodynamic states and the liquid phase residence time, the independence of ϕ on fluid flowrates is not entirely unexpected. It is recalled that the liquid phase is assumed by the hydrodynamic model to flow in rivulets which bridge the packing surfaces in regions where they flow. Stagnant holdup occurs mainly in sheltered regions along the liquid flowpaths, such as crevices between packing particle surfaces. As such, the extent of stagnancy in fractional terms is relatively unaffected by the magnitude of the fluid flowrates which influence holdup only by changing the number of rivulets and varying the liquid velocity in the dynamic

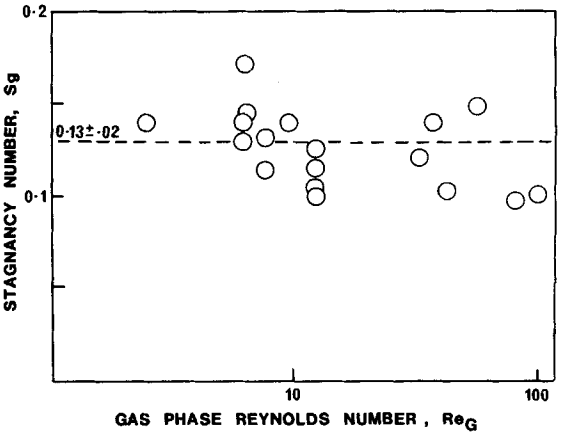

Figure 6. Relationship between Stagnancy number and gas-phase Reynolds number.

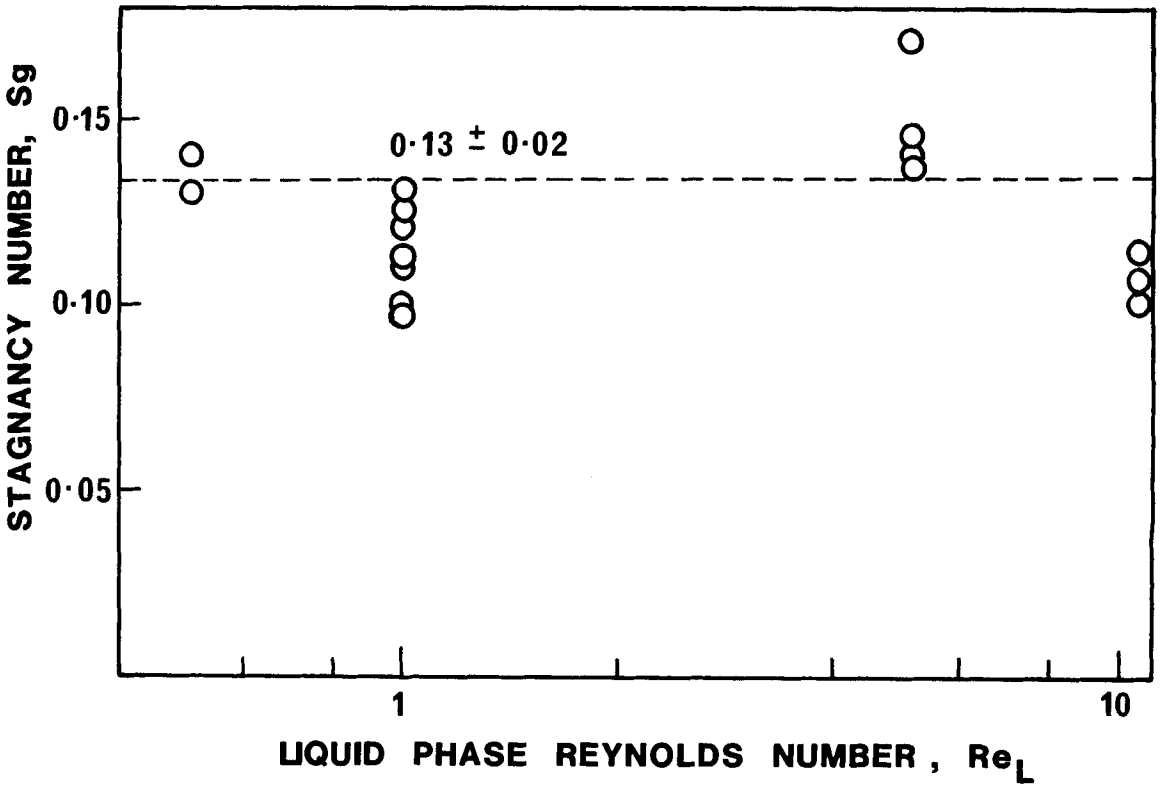

Figure 7. Relationship between Stagnancy number and liquid-phase Reynolds number.

holdup. In other words, the independence of parameter ϕ on liquid flowrates may be taken to be an experimental verification of the rivulet theory in general, and the Stagnancy model in particular.

The estimated magnitude of ϕ (0.73 ± 0.08) agrees well with the results of Matsuura et al. (1976) (0.75 to 0.9). Their work also showed little dependence of ϕ on the fluid flowrates. The agreement was also good with the results of Hochman and Effron (1969) (0.65 to 0.85) although, in their studies, some dependence on flowrate was reported.

In respect of the Stagnancy number defined as

$$Sg = \Delta\sqrt{\frac{\overline{U_L}}{E_s' Z}}$$

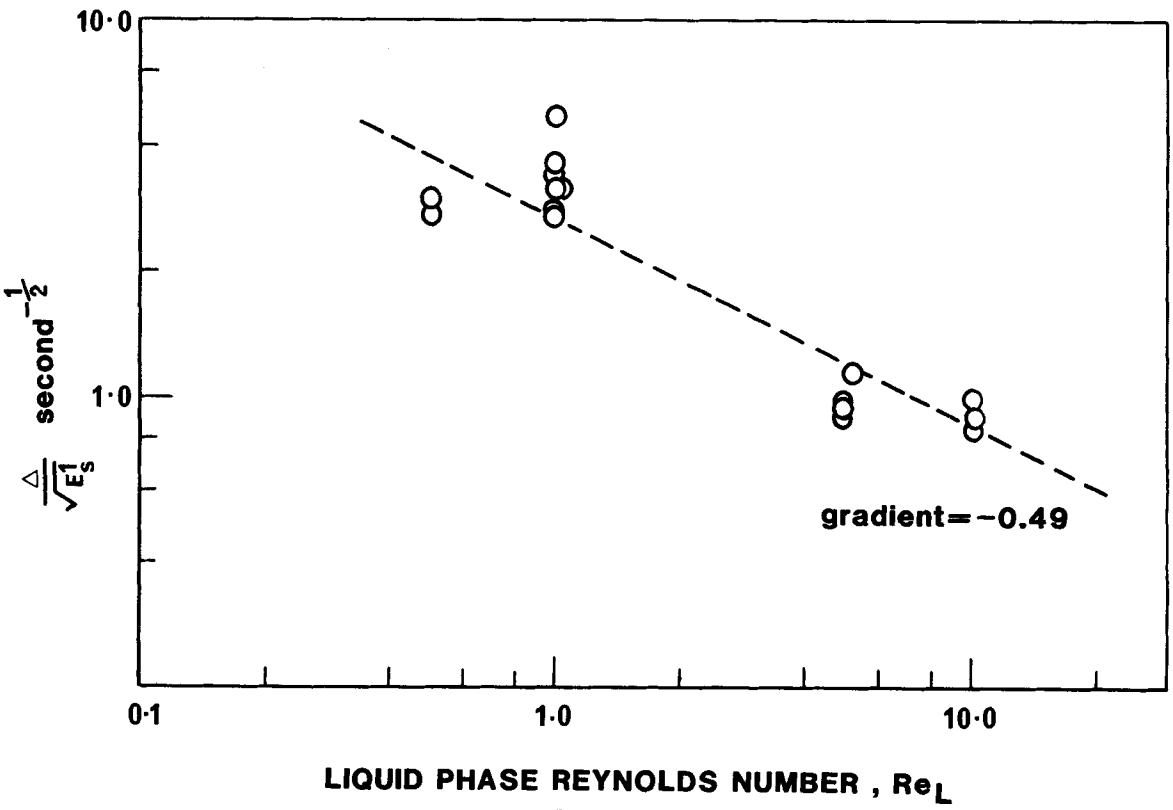

Figure 8. Relationship between $\Delta/\sqrt{E_s'}$ and liquid-phase Reynolds number.

the mean value was 0.13 with a standard deviation of 0.01. The results are plotted in Figures 6 and 7. Although the scatter in the data was greater than in the case of ϕ, it was not sufficient to compensate for the variation in $\overline{U}_L$ used (Re_L ranged from 0.5 to 10.2). It can be shown that, as ϕ was found to be constant, Δ must also be constant and there is no way that E_s' could also be constant when Z was varied only slightly from 0.5 to 0.8 m in the experiments. Thus, E_s' cannot be the molecular diffusivity and the mechanism of mass transfer in the stagnant regions cannot be solely by molecular diffusion. Instead, the explanation for the invariance of Sg could lie in the relationship between E_s' and $\overline{U}_L$. Since E_s' occur together with Δ in the form of $\Delta/\sqrt{E_s'}$, it is not possible to consider E_s' in isolation. Nevertheless, as Δ is constant with respect to the fluid flowrates, the same information is still conveyed when considering $\Delta/\sqrt{E_s'}$ as a whole as in Figure 8. Since the gradient of the relationship is -0.49 it follows that

$$\frac{1}{\sqrt{E_s'}} \propto Re_L^{-0.49}$$

or

$$E_s' \propto Re_L$$

It is interesting to note that this relationship is quite similar to that obtained for the axial dispersion coefficient of single-phase flows through packed beds suggesting that the basic mechanisms are similar. Thus in two-phase flows, dispersion is primarily a mixing process that occurs in the stagnant region, transferring mass to and from the dynamic regions. This is an important observation as it again attributes dispersion to a mixing process rather than a molecular diffusional one.

It has been pointed out that the incorporation of the term E_s' allows for incomplete mixing in the stagnant region which is more realistic than the existing crossflow models such as those of Hochman and Effron (1969), Matsuura et al. (1975) and Bennett and Goodridge (1970), where the mixing in the stagnant regions was considered to be complete. The value of $\Delta/\sqrt{E_s'}$ has been found to lie between 1.0 and 5.0 $s^{-1/2}$. While Δ could not be independently determined, it could be roughly estimated from the geometry of the packing to be in the region of 10^{-4} m, suggesting that E_s' must lie in the region of 10^{-10} $m^2 \cdot s^{-1}$. It is interesting to note that for complete mixing, E_s' would have to be a very large number.

The above observation on the nature of the dispersion was further confirmed with experimental runs carried out with dextran as the tracer for which the Stagnancy number obtained was 0.149 compared to 0.13 for potassium chloride, a difference that was quite negligible. Since dextran T2000 has a mean molecular weight of 2×10^6, it has a molecular diffusivity of ca 5.0×10^{-10} m^2/s or about 1/20 of that of potassium chloride, and the Stagnancy number would have to be 4.5 times greater if molecular diffusion had been the mechanism. Such a great difference was not observed and this lends strong support to the assertion that molecular diffusion must be ruled out as a significant contributor to dispersion in the trickle beds.

ACKNOWLEDGMENT

The assistance provided by the Australian Research Grants Commission is gratefully acknowledged.

NOTATION

a_s = specific interregional area, m^{-1}
A = cross-sectional area of bed, m^2
c = concentration, $kg \cdot m^{-3}$
c = Laplace transform of c
c_d = concentration in dynamic region, $kg \cdot m^{-3}$
c_s = concentration in stagnant region, $kg \cdot m^{-3}$
C = dimensionless concentration as defined in text
D_m = molecular diffusivity, $m^2 \cdot s^{-1}$
E_s' = dispersion coefficient in stagnant region, $m^2 \cdot s^{-1}$
E_z = axial dispersion coefficient based on empty column, $m^2 \cdot s^{-1}$
E_z' = axial dispersion coefficient in dynamic region, $m^2 \cdot s^{-1}$
h_t = total liquid holdup
k_i = ith weighted cumulant
m_i = ith moment
N = mass flux, $kg \cdot m^{-2} \cdot s^{-1}$
Δp = pressure difference, Pa
Q_L = liquid volumetric flowrate, $m^3 \cdot s^{-1}$
Re_L = liquid-phase particle Reynolds number
Re_G = gas-phase particle Reynolds number
$Re_{G_{max}}$ = maximum gas-phase particle Reynolds number experienced by bed
s = weighting factor
Sg = Stagnancy number as defined in text
t = time, s
U_d = liquid-phase velocity in dynamic region, $m \cdot s^{-1}$
$\overline{U}_L$ = liquid-phase superficial velocity, $m \cdot s^{-1}$
y = distance in stagnant region, m
z = distance from top of bed, m
Δ = stagnant film thickness, m
ϵ = bed voidage
μ_L = liquid viscosity, $kg \cdot m^{-1} \cdot s^{-1}$
μ_G = gas viscosity, $kg \cdot m^{-1} \cdot s^{-1}$
ρ_L = liquid density, $kg \cdot m^{-3}$
ρ_G = gas density, $kg \cdot m^{-3}$
ϕ = fraction of liquid holdup that is dynamic

LITERATURE CITED

Anderssen, A. S., and E. T. White, "Parameter Estimation by the Weighted Moments Method," *Chem. Eng. Sci.*, **26**, 1203 (1971).

Bennett, A., and F. Goodridge, "Hydrodynamic and Mass Transfer Studies in Packed Absorption Columns," *Trans. Instn. Chem. Engrs.*, **48**, T232 (1970).

Buchanan, J. E., "Holdup in Irrigated Ring-Packed Towers Below the Loading Point," *Ind. Eng. Chem. Fund.*, **6**, 3, 400 (1967).

Carnahan, B., H. A. Luthers, and J. O. Wilkes, "Applied Numerical Methods," John Wiley (1969).

Davidson, J. F., "The Hold Up and Liquid Film Coefficient of Packed Towers, Part II: Statistical Models of the Random Packing," *Trans. Inst. Chem. Engrs.*, **37**, 131 (1959).

Davidson, J. F., E. J. Cullen, D. Hanson, and D. Roberts, "The Hold Up and Liquid Film Coefficient of Packed Towers, Part I: Behaviour of a String of Spheres," *Trans. Inst. Chem. Engrs.*, **37**, 122 (1959).

Hays, J., "Mass Transport Mechanisms in Open Channel Flow," Ph.D. Thesis, Vanderbilt University, USA (1966).

Hochman, J. M., and E. Effron, "Two-Phase Cocurrent Downflow in Packed Beds," *Ind. Eng. Chem. Fund.*, **8**, 1, 63 (1969).

Hoogendoorn, C. J., and J. Lips, "Axial Mixing of Liquid in Gas-Liquid Flow Through Packed Beds," *Can. J. Chem. Eng.*, **43**, 125 (1965).

Hutton, B. E. T., and L. S. Leung, "Cocurrent Gas-Liquid Flow in Packed Columns," *Chem. Eng. Sci.*, **29**, 1681 (1974).

Kan, K. M., "Modelling of Trickle Bed Reactors with Small Packings—hydrodynamics, residence time distribution and reactor design," Ph.D. Thesis, University of Queensland, Australia (1980).

Kan, K. M., and P. F. Greenfield, "Multiple Hydrodynamic States in Cocurrent Two-Phase Downflow through Packed Beds," *Ind. Eng. Chem. Process Design Dev.*, **17**, 4, 482 (1978).

Kan, K. M., and P. F. Greenfield, "Pressure Drop and Holdup in Two-Phase Cocurrent Trickle Flows through Beds of Small Packings," *Ind. Eng. Chem. Process Design Dev.*, **18**, 4, 740 (1979).

Matsuura, H., T. Akehata, and T. Shirai, "Axial Dispersion of Liquid in Cocurrent Gas Liquid downflow in Packed Beds," *J. Chem. Eng. Japan*, **9**, 294 (1976).

Michell, R. W., and I. A. Furzer, "Trickle Flow in Packed Beds," *Trans. Inst. Chem. Engrs.*, **50**, 4, 334 (1972).

Porter, K. E., and G. K. Stephens, "A Method for Estimating Inter Rivulet

Mixing," *Can. J. Chem. Eng.*, **47**, 258 (1969).
Specchia, V., and G. Baldi, "Pressure Drop and Liquid Holdup for Two-Phase Cocurrent Flow in Packed Beds," *Chem. Eng. Sci.*, **32**, 515 (1977).
Turpin, J. L., and R. L. Huntington, "Prediction of Pressure Drop for Two-Phase, Two-Component Cocurrent Flow in Packed Beds," *AIChE J.*, **13**, 6, 1196 (1976).
White, E. T., "Evaluation of the Zakian Numerical Method for Inverting Laplace Transforms," Automation 77 Conf., Auckland, New Zealand (1977).
Van Swaaij, W. P. M., J. C. Charpentier, and J. Villermaux, "Residence time Distribution in the Liquid Phase of Trickle Flow in Packed Columns," *Chem. Eng. Sci.*, **24**, 1083 (1969).

Manuscript received August 13, 1981; revision received February 23, and accepted March 4, 1982.

Tortuosity Factors for Diffusion in Catalyst Pellets

The dynamic pulse-response technique was used to measure effective diffusivities under nonreacting conditions in two, unsulfided, extrudate-type, hydrodesulfurization catalyst pellets of different porosities. Pore-volume distribution data showed a bidisperse pore structure with a broad pore-size range (100 μm to 3 nm).

The main purpose of the study was to evaluate various methods for calculating the tortuosity factor, τ. For this particular catalyst, the most constant and unreasonable values of τ were obtained by supposing that diffusion occurred in all the pore volume (micro and macropores) and by summing the combined Knudsen and bulk contributions over each increment of pore volume.

CHANG-TAI WANG
and
J. M. SMITH
University of California
Davis, CA 95616

SCOPE

Tortuosity factors τ are a helpful measure of the effects of pore structure on diffusion in catalyst pellets. When pore sizes are small enough for Kundsen diffusion to be significant and when the distribution of pore volume is over a wide range of pore radii, there is uncertainty in how to evaluate τ. When the catalyst pellet is prepared by compressing porous particles, as, for example, for alumina pellets, it has often been assumed that diffusion occurs only in the macroporers surrounding the microporous particles. However, it seems more logical to include diffusion in both micro and macropores. Especially when some interparticle pores are smaller than the largest intraparticle pores (micropores), it is preferable to include the total pore volume in evaluating the tortuosity factor. With respect to Knudsen diffusion, there is the question of the proper pore radius to employ.

The purpose of this paper is to test various methods of evaluating τ, including a new approach based upon summing the combined bulk plus Knudsen contributions over the total pore volume. To evaluate the methods, diffusion data are obtained from 298 to 502 K and at 1 atm for pellets of two densities prepared from an extrudate type of unsulfided hydro-desulfurization catalyst. Measurements were made by the dynamic technique (Dogu and Smith, 1975) for He–N_2 and H_2–N_2 systems, both of which were nonadsorbing. Pore-volume distribution data were also obtained for the two pellets.

CONCLUSIONS AND SIGNIFICANCE

Both pellets exhibited a wide range of pore diameters from greater than 10×10^{-5}m to 3×10^{-9}m. The distribution was bidisperse with nearly the same micropore ($r < 50 \times 10^{-10}$m) distribution (Figures 1 and 2). The chief difference in pore volume was due to elimination of much of the macropore region for the more dense pellet.

As expected, effective diffusivities were substantially less for the more dense pellet even though the porosity was not much less (0.569) than that (0.677) for the less dense pellet. Tortuosity factors were higher when diffusion was assumed to occur only in the macropore ($r > 50 \times 10^{-10}$m) region. In fact, τ was unreasonably large (14 to 45) except when the pore radius for Knudsen diffusion was taken to be a constant value calculated from the macropore volume and surface area according to the equation $2(V_g)_m/(S_g)_m$. If diffusion is assumed to occur in all

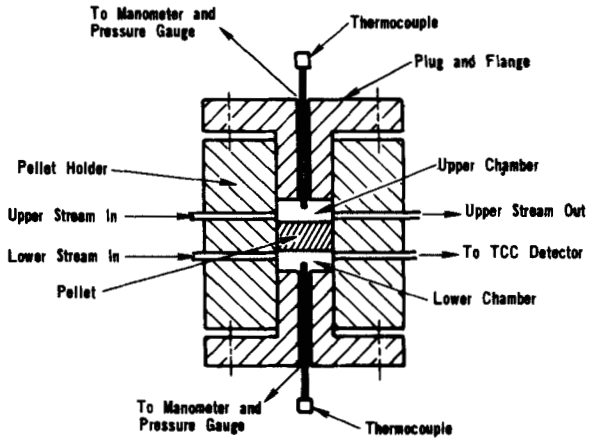

Figure 1. Schematic drawing of diffusion cell.